Jurnal Teknologi

Full Paper

FINITE ELEMENT SIMULATION OF LOW-RISE SCHOOL BUILDING MODEL WITH SEISMIC LOADS INPUT

Jet-Wei Pang[a], Chun-Chieh Yip[a]*, Lloyd Ling[a], Jing Ying Wong[b], Foong Sin Lam[a], Chee Fui Wong[a]

[a]Department of Civil Engineering, Universiti Tunku Abdul Rahman, Bandar Sungai Long, 43000, Cheras, Kajang, Selangor, Malaysia
[b]Department of Civil Engineering, University of Nottingham Malaysia Campus, 43500, Semenyih, Selangor, Malaysia

Article history
Received
23 January 2024
Received in revised form
22 May 2024
Accepted
22 May 2024
Published Online
17 October 2024

*Corresponding author
yipcc@utar.edu.my

Graphical abstract

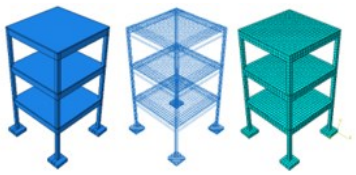

Abstract

Earthquake impacts on buildings have garnered increased attention as Malaysia experiences seismic activities, notably from nearby regions like Sumatra and within areas such as Sabah. Despite this, current Malaysian design guidelines, such as BS 8110, do not fully incorporate seismic loads. This study addresses this gap by examining the structural performance of a scaled 1:8 model of a three-storey, low-rise school building under various peak ground accelerations (PGA) from 0.1g to 1.0g. Utilizing ABAQUS finite element simulation and time-history analysis, we evaluated the seismic responses, including local deformations, von Mises stress, and principal stresses. Key findings reveal a maximum structural displacement of 10.22 mm at 1.0g PGA, with significant stress concentrations observed at the column footings, highlighting critical areas for design improvement in seismic resilience.

Keywords: Low-rise building, Finite element simulation, ABAQUS, scaled model

Abstrak

Kesan gempa bumi terhadap bangunan di Malaysia, khususnya dari kawasan berhampiran seperti Sumatra dan Sabah, semakin mendapat perhatian. Namun, garis panduan reka bentuk semasa seperti BS 8110 tidak sepenuhnya mengambil kira beban seismik. Kajian ini menilai prestasi struktur model berskala 1:8 bangunan sekolah rendah tiga tingkat dengan pelbagai pecutan tanah puncak (PGA) dari 0.1g hingga 1.0g menggunakan simulasi elemen terhingga ABAQUS. Hasil kajian menunjukkan anjakan maksimum 10.22 mm pada 1.0g PGA, dengan tumpuan tegasan pada tapak tiang, menonjolkan keperluan untuk penambahbaikan daya tahan seismik.

Kata kunci: Bangunan rendah, Simulasi elemen terhingga, ABAQUS, model berskala

1.0 INTRODUCTION

In recent years, the increasing frequency and impact of seismic events near Malaysia, particularly in regions like Sabah and due to activity in the Sumatra area, have propelled the study of earthquake impacts on buildings to the forefront of civil engineering research. Despite the proximity to seismic zones, Malaysian design guidelines, notably BS 8110, remain deficient in integrating comprehensive seismic load

considerations. This study addresses this critical gap by evaluating the seismic resilience of low-rise school buildings—a structure typology common across Malaysia yet overlooked in seismic assessments. Utilizing advanced finite element simulation through ABAQUS, this research not only tests the existing guidelines but also proposes an enhanced analytical model that provides deeper insights into structural behaviours under varied seismic intensities. This novel approach highlights the need for revising current standards to better safeguard infrastructure against potential seismic threats, offering a significant contribution to both academic research and practical engineering applications in seismically active regions.

Malaysia is located near the boundary of the two most active plates. The boundaries between these two plates are the inter-plate boundary between the Philippine Plate and the Eurasian Plate in the east, and the inter-plate boundary between the Indian-Australian Plate and the Eurasian Plate in the west. As these plates move westward at any time, it is reasonable to assume that Malaysia may also have a high risk in the danger of earthquakes [4]. To date, Malaysia has not experienced any catastrophic earthquakes, but the country has experienced the damage caused by earthquake such as tsunamis [5].

According to Doocy, *et al*., 2016 [6], the main reason of death related to the earthquake was the collapse of buildings, which most often resulting in soft tissue damage, ruptures and crush damages. Because of the population growth in an area with high-risk earthquakes and low development, as well as insufficient building quality, the earthquake losses are expected to be increased in the next few years. However, changes in the structural performance under additional loads such as seismic loads, were not considered in the design guideline in Malaysia such as BS 8110 [7]. Most of the tremors have occurred in low populated area therefore people have not paid too much attention to face the panic and damage caused by earthquakes.

Assume that the infrastructure damaged by the earthquake is a school building, the lives of young people will be severely at risk. Their safety and continuous education are extremely important, not only for parents, but also for the country's long-term social development and economic prosperity. It is essential to consider this issue when designing the structure to avoid causing damage or collapse to the building.

Due to the height factor, the seriousness of the collapse of the low-rise building was underestimated in most of the countries. Many low-rise reinforced concrete buildings have been constructed with significant structural deficiencies that have resulted in greatly reduced expected seismic safety. These buildings generally have low concrete compressive strength and severe corrosion can be observed in some of the parts. Therefore, these buildings will be severely damaged or immediately collapsed once they are hit by the predictable earthquake [8]. Hence, earthquake code requirements must be followed during the construction of buildings so that the buildings can provide the level of performance specified in the code to encounter earthquakes.

In order to study the seismic performance of a building, a school which is a low-rise building was selected for modelling by using finite element analysis software. Besides, with the purpose of getting more accurate results, ABAQUS software is selected to simulate the structure. It is believed that the impact of the earthquakes can be greatly reduced if the advantages of software is fully utilized.

Finite element analysis (FEA) software is considered a powerful tool for engineering analysis to solve dynamics problems for various conditions including solid, liquid and gas, by considering the linear and non-linear behaviour of materials [9]. Moreover, it is not only to help engineers to discover solutions earlier in the design cycle, saving time and money, but also provide insights on how to improve quality before physical prototyping [10]. In addition, by predicting the machining parameters such as cutting force, chip formation and temperature distribution, the causes of the failure can be identified and thus the failures can be avoided [11]. As a result, the productivity and the quality of machined parts, as well as machining performance can be improved.

ABAQUS is one of the well-known engineering simulation computer software which is first established by Dassault Sustèmes in 1978 [12]. It has a wide range of capabilities for analysing finite element problems including linear and nonlinear analysis of structures. ABAQUS is able to model any geometry because it has a broad library of elements [13]. The performance of a structure can be observed by implementing the three-dimensional finite element model using ABAQUS. In addition, ABAQUS is a universal simulation tool that able to resolve a numerous area of problem such as heat transfer, acoustics, automotive and mechanical issues as well as to stimulate and study the explosion phenomena and wave propagation [14].

Many researchers have conducted studies to investigate the seismic performance of RC buildings. For instance, Melani, *et al*., 2016 [15] conducted the seismic assessment of typical low-rise reinforced concrete frames, where the design concepts of the capacity of the three frames are analysed, which included the shear capacity, flexural capacity and contribution of floor reinforcement and beams. Maximum inter-storey drift ratios obtained from the time-history analyses are plotted against the intensities of ground motion. In addition, according to the nonlinear analysis of earthquake-induced vibration conducted by Vlad Inculet [16], the earthquake loads are applied to the element's surface by means of accelerograms and the performance of displacement of the structure's top will be compared. The analysis is completed in ABAQUS for all types of materials, geometries and earthquake loading. Besides, two different accelerograms are applied to the support separately in this analysis, which are North-South acceleration component of California's 1940 El

Centro earthquake and North-South component of Romania's 1977 Vrancea earthquake. For a three-dimensional column, the maximum normal stress is at the base of the column for both earthquakes. Whereas for a multi-storey frame concrete structure, the displacement on storey one is much higher than upper storey,

The present study conducts a whole new simulation work as no one has done this simulation before. This study is crucial to simulate structural behaviour of a seismic loaded downscaled one bay three storeys reinforced concrete school building as it is evaluated in the face of an earthquake. The local deformation of the member and the stress concentration on critical members will be evaluated under prescript seismic loads by using ABAQUS finite element simulation software. This research is very useful in enhancing the designer's understanding of the interaction between the low-rise building and seismic loads. The results of the experimental data can be served as a reference to identify the structural behaviour of the low-rise building under prescript seismic loads with PGA 0.1g, 0.16g, 0.3g, 0.5g, 0.7g, 0.9g and 1.0g. Besides, the results also can be used as a reference for engineers when further studying the new building design standards.

2.0 METHODOLOGY

2.1 Material Properties

In this study, a reinforced concrete building was modelled using Class C25/30 concrete grade for the structure. Therefore, the concrete's characteristic material strength applied to the structure is fck = 25 N/mm^2 [17]. Besides, steel grade S275 is used so the characteristics material strength is fyk = 275 N/mm^2 for the steel [18]. The list of material properties for concrete and reinforcement bar is summarized in Table 1. ABAQUS is consistent in units so the units in this study are all in millimetres, Newton and tonne [19].

Table 1 The Summary of the Material Properties

Grade C25/30 Concrete	
Mass Density, tonne/mm^3	2.4 x 10^{-9}
Young's Modulus, N/mm^2	30 000
Poisson's Ratio	0.2
Dilation Angle, °	31
Eccentricity	0.1
f_{b0}/f_{co}	1.16
k	0.667
Compression yield stress, N/mm^2	25
Tension yield stress, N/mm^2	2.25

Grade S275 Steel	
Mass Density, tonne/mm^3	7.85 x 10^{-9}
Young's Modulus, N/mm^2	210 000
Poisson's Ratio	0.3
Yield stress, N/mm^2	275

2.2 Section Properties

Figure 1 shows the three storeys reinforced concrete structure and Figure 2 represents the cross sections of the construction elements such as beams, columns and foundations as modelled in AutoCAD. This is a scaled 1:8 model. The total height of the building is 1500 mm. Concrete covers of the reinforcement for the column and beam are taken as 5 mm. The summarized of the section properties of the scaled structure is shown in Table 2. Meanwhile, Figure 3 shows the reinforcements of column, beam, slab and footing respectively.

Table 2 Section Properties of the Scaled Structure

Structural Element	Dimension (mm)	Reinforcement
Column	40 x 40	8T3
Beam	31 x 75	4T3
Slab	830 x 830 x 16	T3-35
Footing	175 x 175	T3-10

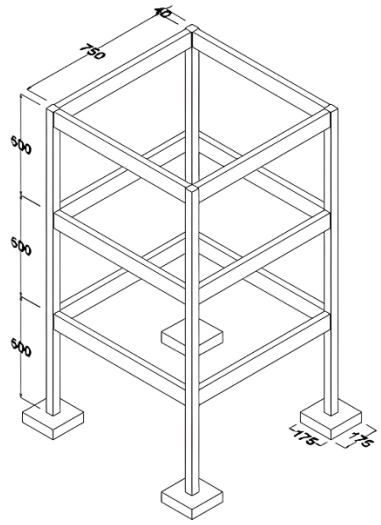

Figure 1 Three-Dimensional View of Structure

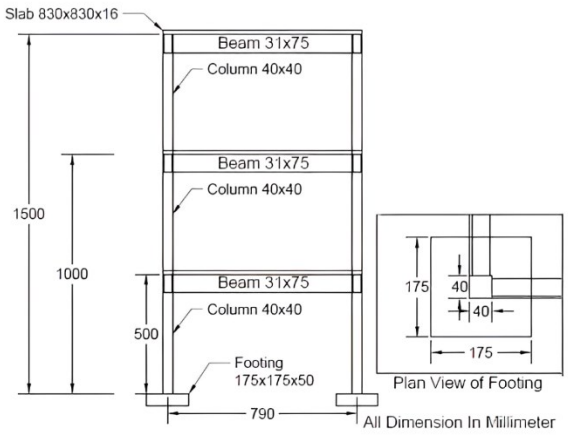

Figure 2 Cross Section of the Building

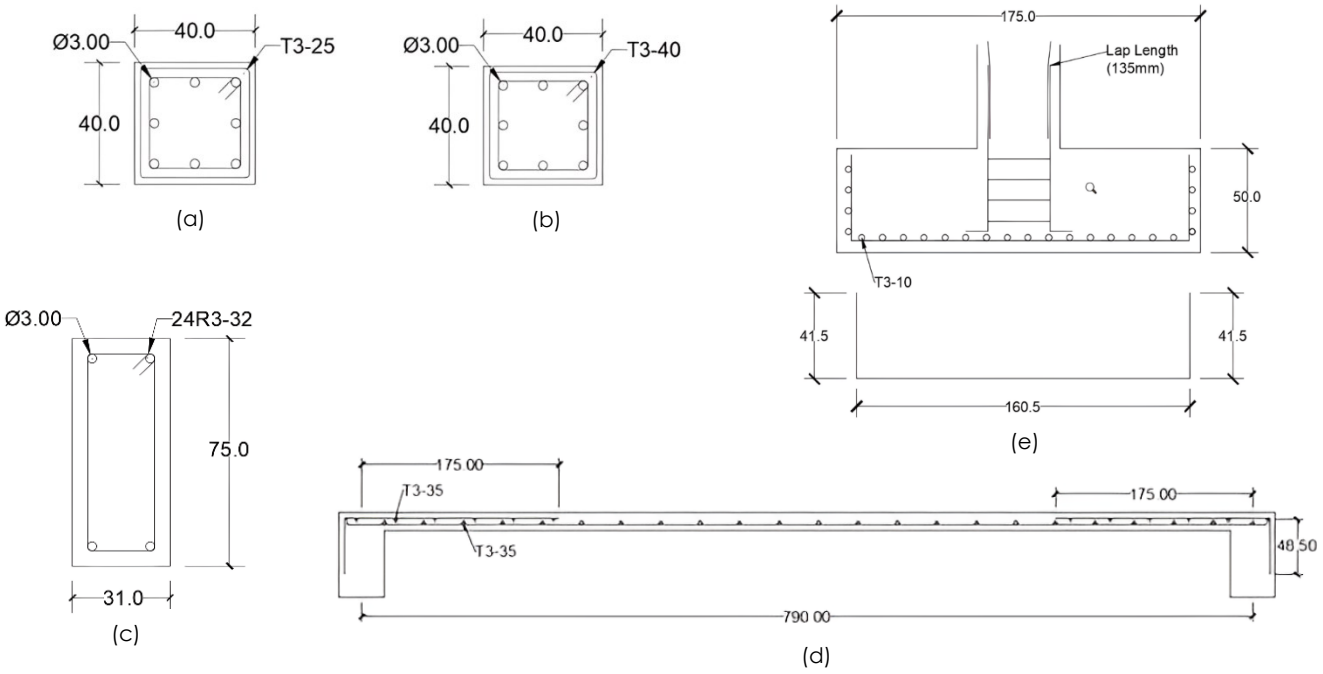

Figure 3 Detailing of (a) Column for Third and Second Floor, (b) Column for First Floor, (c) Beam, (d) Slab & (e) Footing

2.3 Earthquake Input Motion

An actual earthquake accelerogram is chosen as the input loads in this simulation. Particularly, the accelerogram recorded at El Centro during 1940 earthquake was utilized in this study [20]. By referring to earthquake disaster map of Malaysia, the peak ground acceleration (PGA) value of Peninsular Malaysia is in the range of 0.02g to 0.10g for 500-year return period. For the same return period, East Malaysia (Sabah and Sarawak) has a higher PGA value which is in the range of 0.06g to 0.12g [21]. In order to cover the wide range of PGA in Malaysia and assess the greater disasters that may occur in the future, few values of PGA had been selected as reference PGA.

As part of this study, each El Centro earthquake input motion was scaled to produce input motions with PGA of 0.1g, 0.16g, 0.5g, 0.7g, 0.9g and 1.0g; thus, up to six sets of El Centro earthquake motions were derived from the accelerogram and used to simulate the structure. The time step of the original El Centro earthquake recording was 0.02 s, but the time step is squeezed to 0.002 s for the simulation. The acceleration time history of the input motions is plotted in Figure 4. The peak acceleration for the motion shown in the figure is approximately 0.3g.

In this study, the El Centro earthquake data was selected as the primary seismic input for the simulations. This choice was strategically made to mirror the potential seismic conditions in Malaysia, particularly in light of the recent seismic activities in regions such as Sabah. The El Centro earthquake is considered a suitable analog due to its relevant seismic characteristics, providing a practical and applicable dataset for assessing structural responses under similar seismic conditions that could occur in Malaysia. This approach ensures that the findings are directly useful for local engineers in designing safer, more resilient structures.

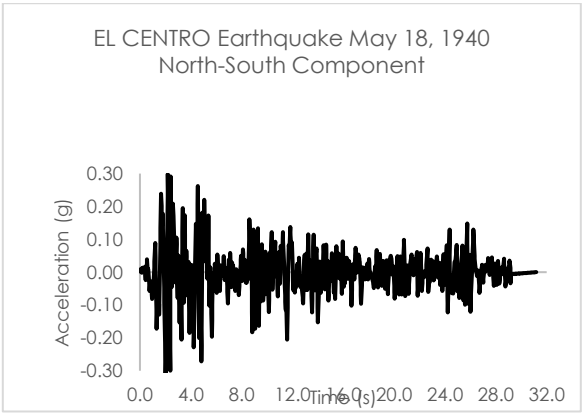

Figure 4 Time History Record of El Centro Earthquake

2.4 Finite Element Simulation Procedures

In this section, a downscaled one bay three storeys reinforced concrete school building is used as an example. Based on all parameters and variables discussed on the previous sub-sections, the structure is modelled by using ABAQUS. Figure 5 illustrates the general work flow chart of this study. The analysis of structural components was conducted using Abaqus finite element software. This involved detailed simulations to assess the response of beams, columns,

and slabs under the applied loads. Parameters such as material properties, geometry, and boundary conditions were defined to closely mimic real-world conditions. The simulation process enabled an in-depth examination of how different structural elements behave under various loading scenarios. The current study focused on the structural response of low-rise school buildings under seismic loads without considering soil-structure interaction (SSI). This assumption was based on the premise that the primary structural response could be effectively analysed assuming fixed base conditions, which simplifies the computational model and focuses on the building behaviour independent of foundation effects. While this approach facilitates clearer insights into the structural dynamics, it is recognized that in real-world scenarios, SSI can significantly influence the seismic response, particularly in buildings situated on softer soil profiles.

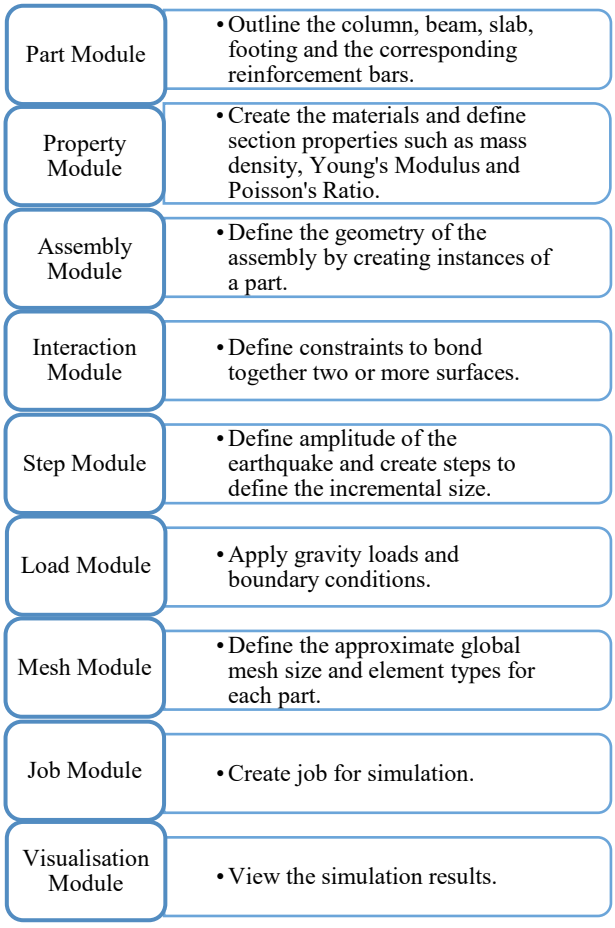

Figure 5 Work Flow Chart of the Study

First, the parts including column, beam, slab, footing and corresponding reinforcement bars are sketched out. The coordinates for concrete parts and the depth are listed down in Table 3 and the coordinates for the lines are listed down in Table 4. An extruded column, beam, slab and footing will be shown in the viewport as presented in Figure 6 to Figure 9 respectively.

Table 3 Coordinates and Depth of the Concrete Parts

Parts	Starting Corner	Opposite Corner	Depth
Column	(0,0)	(40,40)	500
Beam	(0,0)	(31.75)	750
Slab	(0,0)	(830,830)	16
Footing	(0,0)	(175,175)	50

Table 4 Coordinates of the Reinforcement Bars

Reinforcement bar	Starting Point	Following Point(s)
Column	(0,0)	(0,500)
Beam	(0,0)	(0,750)
Slab	(0,0)	(830,0)
	(0,6)	(175,6)
	(665,6)	(830,6)
Footing	(0,41.5)	(0,0), (160.5,0), (160.5,41.5)

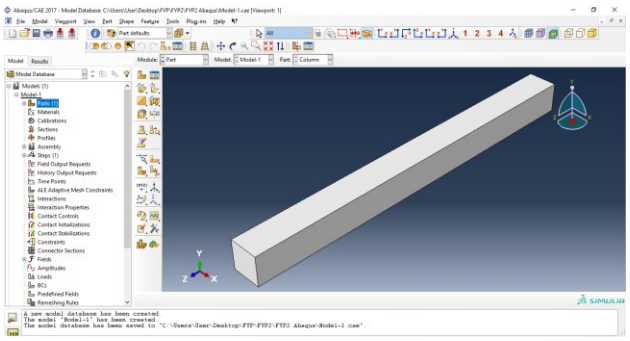

Figure 6 Extruded Concrete Column Model

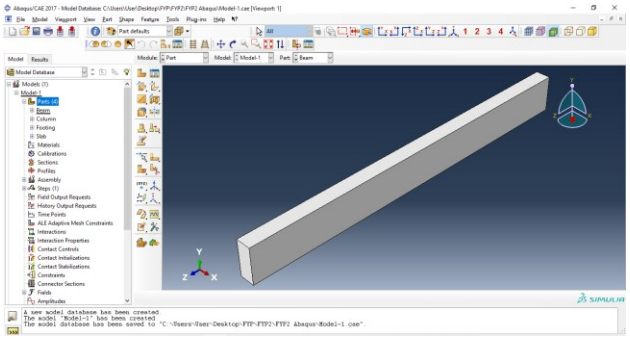

Figure 7 Extruded Concrete Beam Model

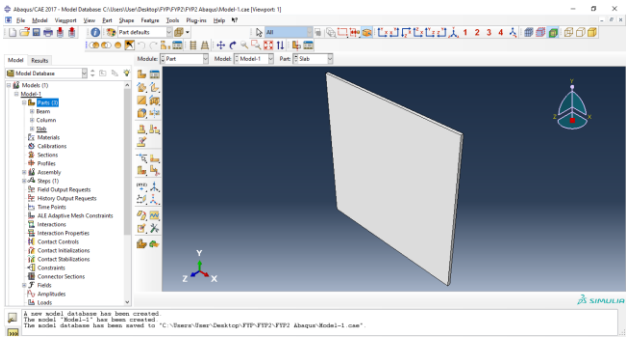

Figure 8 Extruded Concrete Slab Model

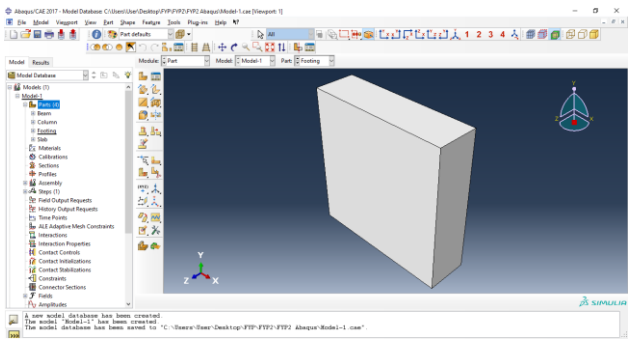

Figure 9 Extruded Concrete Footing Model

Then, the materials such as reinforced concrete and steel are created by defining the material properties, for example: Mass Density, Young's Modulus and Poisson Ratio. Besides, the section properties of reinforced concrete and steel are also created and assigned to the model respectively. The material of concrete model and reinforcement bar will be defined by following the material properties stated at Section 2.1 previously.

The model is now ready for assembly. Connection details between structural elements are modelled to reflect realistic behaviour under seismic loads. Beam-to-column joints are crucial in the structural integrity of frame systems during earthquakes. In the model, these connections are assumed to be rigid to simplify the analysis while capturing the effect of moment transfer between beams and columns. Each part created previously not only has different direction depends on the own coordination system, but also independent of other parts in the model. A model contains only one assembly although the model may contain many parts. The geometry of the assembly can be defined by generating the instances of a part and make a relation to the instances in a global coordinate system. There are two types of instance which are independent and dependent part instances. The difference between independent and dependent part instances are independent part instance mesh separately whereas the mesh of the dependent part instance is linked with the mesh of the original part. Figure 10 to Figure 13 show the wireframe render model.

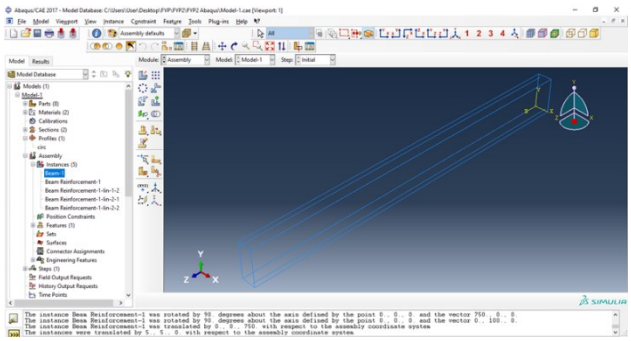

Figure 10 The Wireframe Render Model of Beam

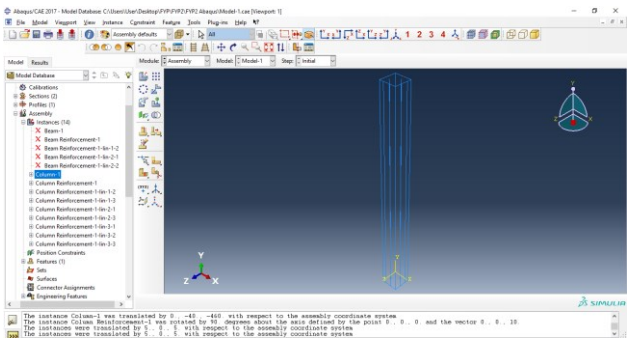

Figure 11 The Wireframe Render Model of Column

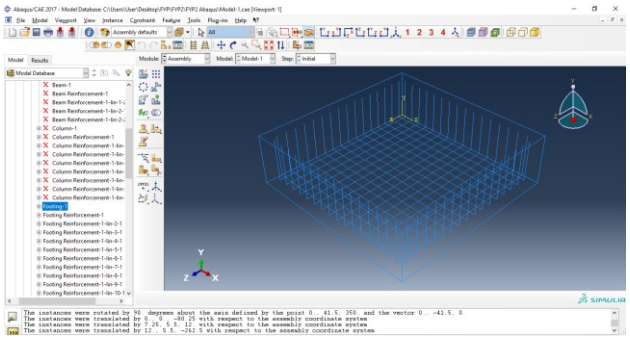

Figure 12 The Wireframe Render Model of Footing

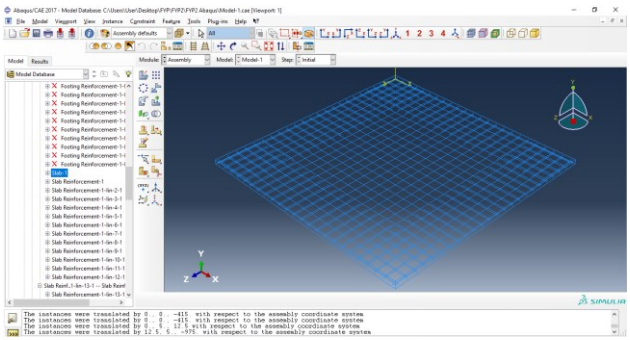

Figure 13 The Wireframe Render Model of Slab

In the finite element model, boundary conditions play a crucial role in simulating the physical behaviour of the structure under load. The base of the columns in the model is fixed to simulate the effect of the foundation, ensuring that all degrees of freedom at the base are constrained. This represents a fixed support condition typically used in seismic analysis to model ground stability. Then the constraints are defined to bond together two or more surfaces. Tie constraint allow to fuse two regions together even though the meshes created on the surface of the region may be different; whereas embedded region constraints allow to embed the area of the model within the "host" region of the model. Figure 14 presents the tie constraints and embedded region constraint.

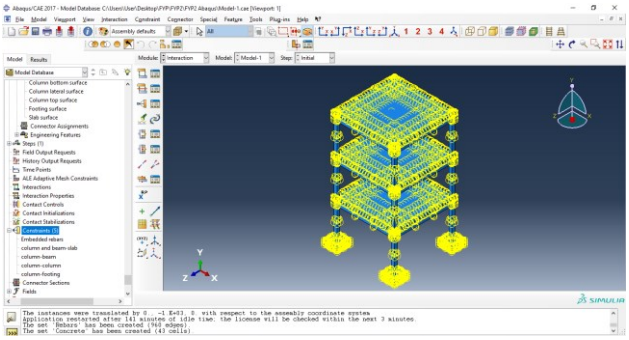

Figure 14 Tie Constraints and Embedded Region Constraint

After the constraints have been created, the analysis can be configured by creating the analysis step. There are two steps in this analysis which are initial step and analysis step. The initial step will be generated automatically by applying boundary conditions while analysis step is needed to be generated by applying the loads. Before creating the analysis step, the time and amplitude of El Centro earthquake are needed to be inserted. Then generate an analysis step by entering the initial incremental size of 0.002 as well as maximum number of increments of 311 800.

The most important step is applying the loads and boundary conditions as the aim of this study is to observe the behaviour of the building under prescript seismic loads. In this study, unidirectional input excitation was selected for seismic simulation. This choice was driven by the need to simplify the analysis focus on the primary axis of structural vulnerability, align with regional seismic activity characteristics, and ensure consistency with common engineering practices in earthquake-prone areas. Additionally, this approach enhances the efficiency of simulations, making it feasible to conduct extensive parametric studies to optimize design recommendations. Figure 15 shows the arrowheads that indicates the boundary conditions created on the bottom of the column and footing.

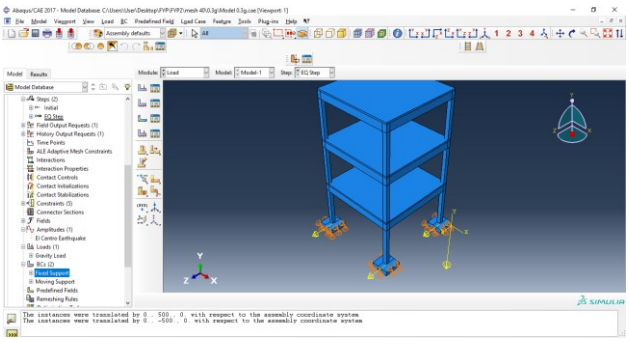

Figure 15 Boundary Conditions

The structural analysis included various types of loads, including standard dead and live loads as specified in EN 1991-1-1, part of Eurocode 1, which outlines general actions on structures. Additionally, seismic loads based on regional seismicity data were considered, adhering to the provisions of EN 1998-1, Eurocode 8, which details the design of structures for earthquake resistance.

The meshing process can be carried out after the model is completed. The meshed model is as illustrated in Figure 16. Finally, analysis job can be made after meshing the model. [22].

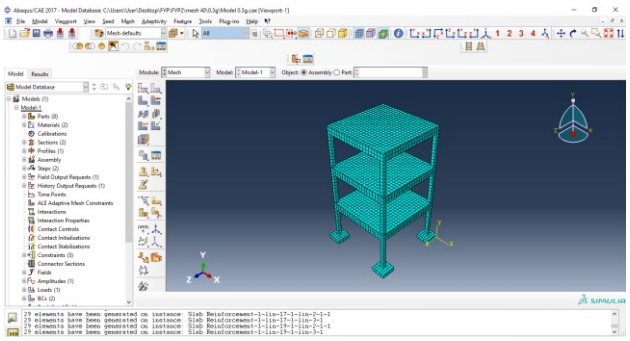

Figure 16 Meshed Model

3.0 RESULTS AND DISCUSSION

3.1 Displacement of the Model

The primary objective of this study is to identify the local deformation of structural members under prescribed seismic loads. Lateral displacement is significant when the structure is subjected to lateral loads such as earthquake loads [23], which is in z-direction. The maximum displacement is indicated as red colour region whereas the minimum displacement is indicated as blue colour region.

Figure 17 depicts the locations of the maximum displacement in z-direction and Figure 18 shows the graphical presentation of the maximum displacement of the model with PGA 0.1g, 0.16g, 0.3g, 0.5g, 0.7g, 0.9g and 1.0g. Besides, Figure 19 indicates the graph of time versus displacement at particular node with maximum displacement.

Referring to the results obtained from the spectrum of different colour contour, the structure with PGA of 1.0g was characterized by greatest displacement, with the ultimate displacement of 10.22 mm. The lateral displacement of the structure increases from 1.027 mm at 0.1g PGA to 10.22 mm at 1.0g PGA in the z-direction. A trend can be observed through the comparison of structure with various PGA in terms of lateral displacement as presented in Figure 18. Structure with lower PGA results in lower lateral displacement comparing to structure with higher PGA. In a nutshell, the value of PGA increases, the roof displacement also increases.

In short, PGA is the measure of how intense the earth vibrates at a particular geographic region. Increasing value of PGA means the earth shakes even harder and greatly displaces the foundation and

lower levels of the structures. Ultimately, shock waves are transmitted through the rest of the structure and causing the building to vibrate back and forth. Also, high PGA value can cause high susceptibility to liquefaction of soil [24], which indicates that the soil is no longer possessed with the strength to retain the building, and this further indicates that the footing of the building is no longer being fixed to the ground. Eventually, the building is in a "floating" state as the soil has lost its strength to maintain the position of the building and thus, the building may deform or collapse accordingly.

Additionally, as Figure 19 implies, the top displacement time-history curves in z-direction of PGA 0.1g, 0.16g, 0.3g, 0.5g, 0.7g, 0.9g and 1.0g are basically in coincidence. It is observed that the displacement vs time period graph from Figure 19 obtained is similar to that of acceleration vs time period graph obtained from earthquake data (Figure 4), reflecting the phenomenon that the amplification coefficient increased with the increase of the depth [25]. Validation of the numerical model is achieved by comparing the simulation results with published data on similar structures subjected to seismic loads. This comparison involves checking the displacement responses and stress distributions against those observed in empirical studies, ensuring that the model accurately reflects the expected physical behaviour. Similar studies, such as the work by Raheem *et al*. (2018), have utilized three-dimensional finite element models to assess seismic response in structures with complex configurations, validating their models against observed seismic demands such as story drift and torsional effects. This comparative framework supports the robustness of the validation approach adopted in this study. [30]

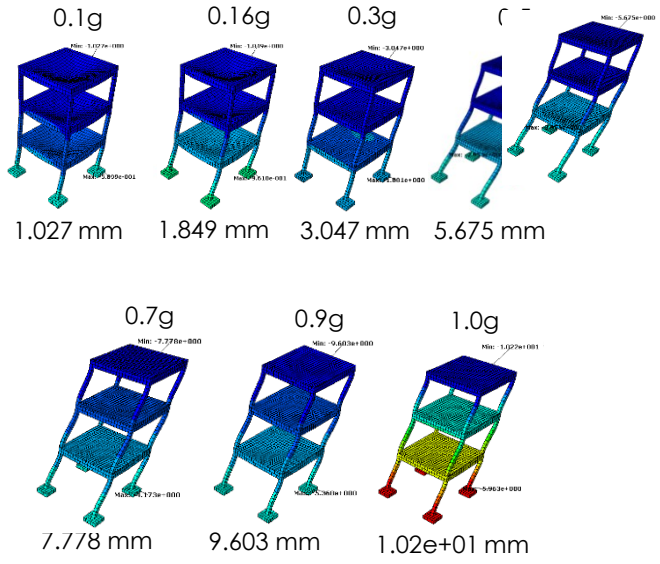

Figure 17 Maximum Displacement of the Model

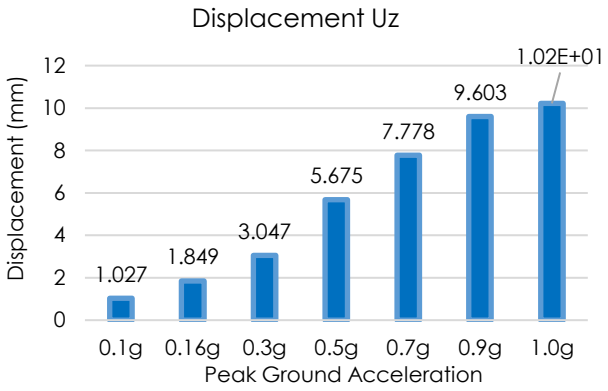

Figure 18 Maximum Displacement in z-direction

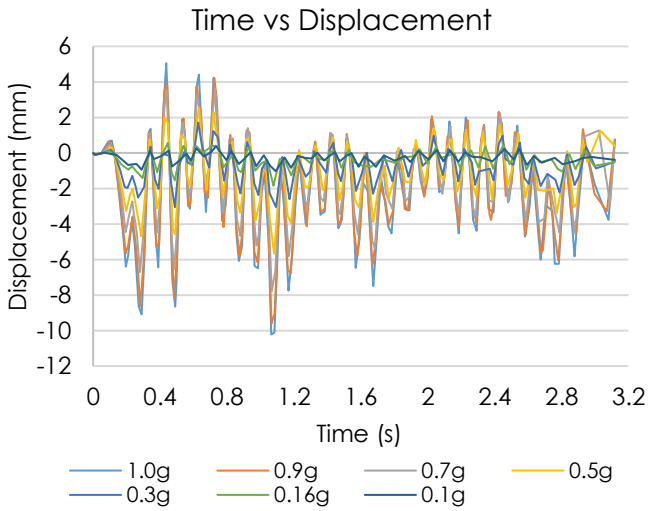

Figure 19 Graph of Time vs Displacement at Particular Node with PGA 0.1g, 0.16g, 0.3g, 0.5g, 0.7g, 0.9g and 1.0g

3.2 Von Mises Stress of Reinforcement Bars

Von Mises stress is a scalar stress measure. Von Mises stress is used in determining the yielding of an isotropic and ductile metal when subjected to a complex loading situation. This can also be checked as an overall indicator of stress distribution and location of stress concentration [26].

The von Mises stress distribution under prescript seismic loads is clearly illustrated in the results adopted from ABAQUS software in Figure 20. Based on Figure 20, it is observed that the maximum stress all occurs in column reinforcement close to the support. The high stress concentration is initiated by the compressive force [27], in which physical forces act inwards on the reinforcement bar, causing it to become compacted.

The simulation results of von Mises stress of reinforcement bars are summarized in Table 5. A trend also can be observed through the comparison of structure with various PGA in terms of von Mises stress as presented in Figure 21. From the figure, it is noticed that the response value of von Mises stress increases

with the increase in PGA value, up to 0.9g, and decreases slightly at 1.0g. Increasing PGA value indicates that the earth agitates the structure more intensively, thus introducing complex forcing function into the structure with the seismic loads. As a result, the ductile reinforcement bars response to the higher PGA value with higher value of von Mises stress. Yet, the von Mises stress obtained at PGA of 1.0g is slightly lower than that of the 0.9g, it may be due to the great deformation of the structure, to the extent that its physical profile has become different with those structure simulated at PGA value of 0.1g to 0.9g. This causes redistribution of the stress in this newly form of structure, and the maximum von Mises stress for PGA value of 1.0g is being diverted to another joint of the structure.

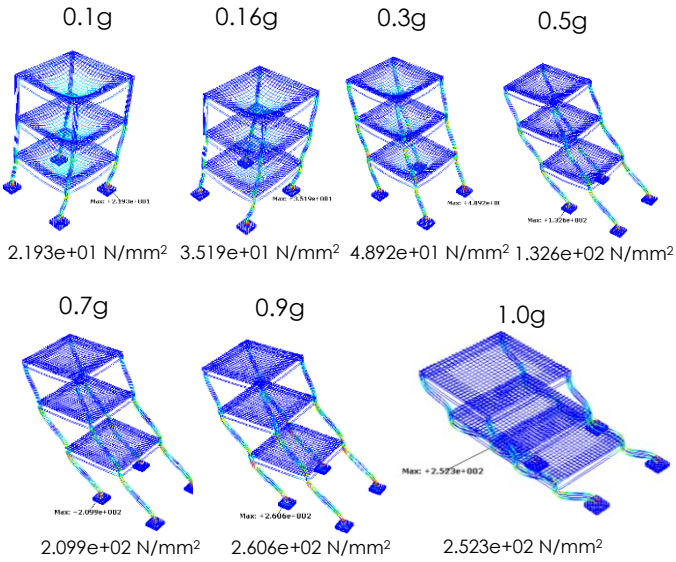

Figure 20 Maximum Displacement of the Model

Table 5 Maximum Von Mises Stress of Reinforcement Bars

Maximum Von Mises Stress, N/mm²		
0.1g	2.193e+01	Column Reinforcement-1.1 Node 1
0.16g	3.519e+01	Column Reinforcement-1.1 Node 1
0.3g	4.892e+01	Column Reinforcement-1.lin-3-1.1 Node 1
0.5g	1.326e+02	Column Reinforcement-1.1 Node 1
0.7g	2.099e+02	Column Reinforcement-1.1 Node 1
0.9g	2.606e+02	Column Reinforcement-1.lin-3-1.1 Node 1
1.0g	2.523e+02	Column Reinforcement-1.lin-1-2-1.11 Node 12

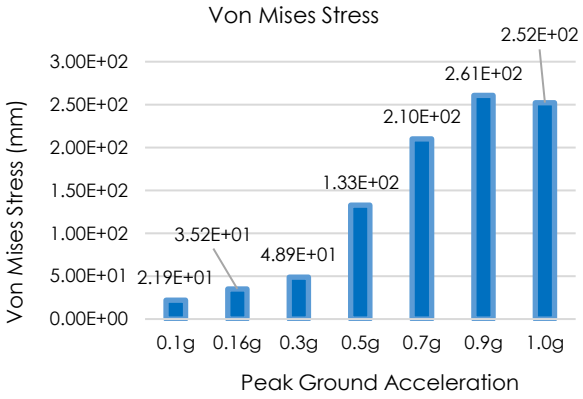

Figure 21 Comparison of Von Mises Stress

3.3 Principal Stresses of Concrete

One of the critical parameters to be taken into account is the principal stresses of the concrete. The principal stresses are the normal stress components in three directions, x direction, y direction and z direction, denoted as S11, S22 and S33. These stress components represent the greatest values of the normal stresses' potential in the material, which are maximum normal stress (major principal stress) and minimum normal stress (minor principal stress) [28].

Figure 22, Figure 23 and Figure 24 illustrate the contour diagrams of principal stresses of concrete. Moreover, Figure 25, Figure 26 and Figure 27 present the graphical presentation of principal stresses whereas Table 6 to 8 list down the major and minor principal stress in x-direction, y-direction and z-direction respectively. Furthermore, Figure 28 summarises the principal stresses of the concrete. As the comparison shown in Figure 28, the greatest principal stress results in z direction. Followed by principal stress in y direction and x direction.

For principal stress in z direction, it is noticed that the response value of principal stress increases with the increase in PGA value up to 0.9g, and then decreases slightly at 1.0g. This may be due to the great displacement of the structure which causes difference of the physical configuration of the structure to those of the structures simulated under PGA 0.1g to 0.9g. As an outcome, the stresses within the structure are redistributed.

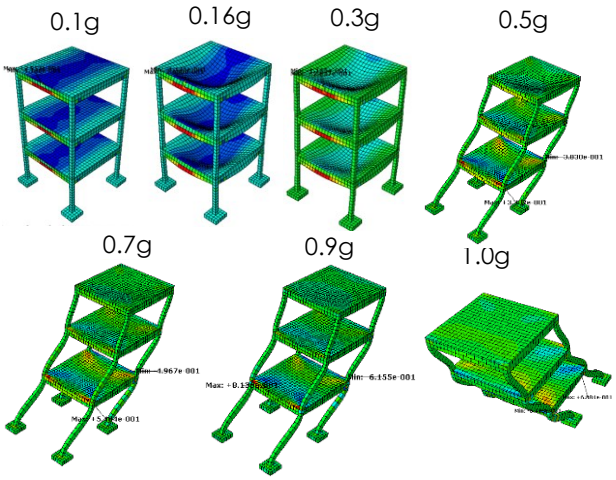

Figure 22 Principal Stress in x direction

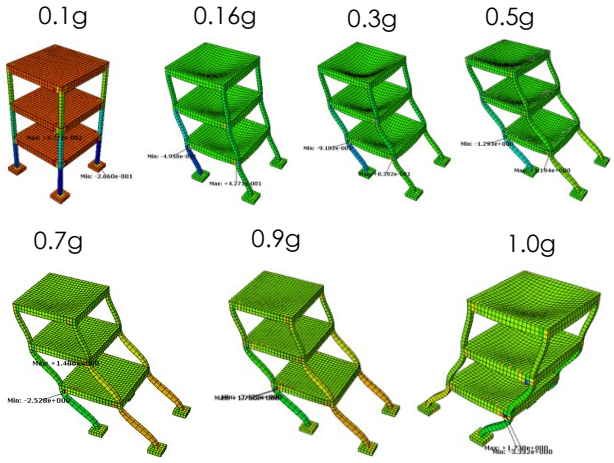

Figure 23 Principal Stress in y direction

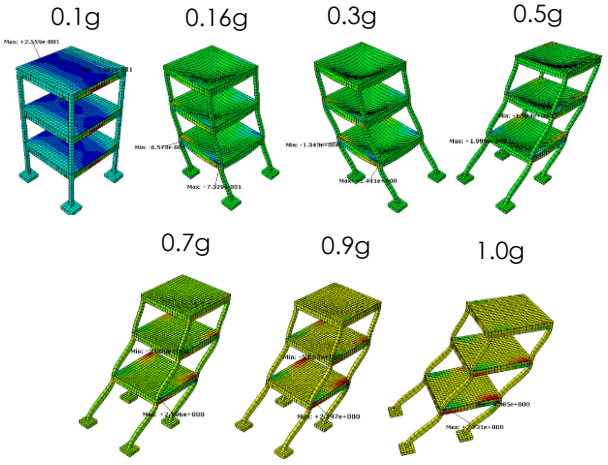

Figure 24 Principal Stress in z direction

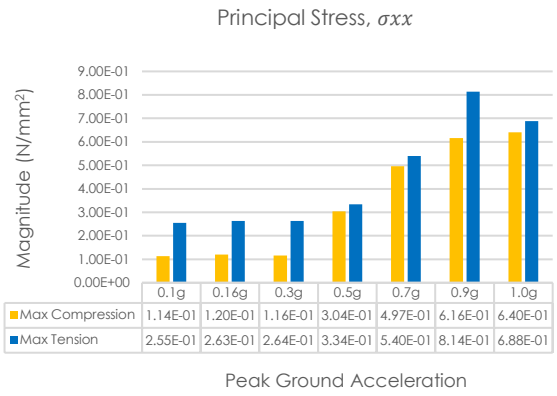

Figure 25 Principal Stress in x direction

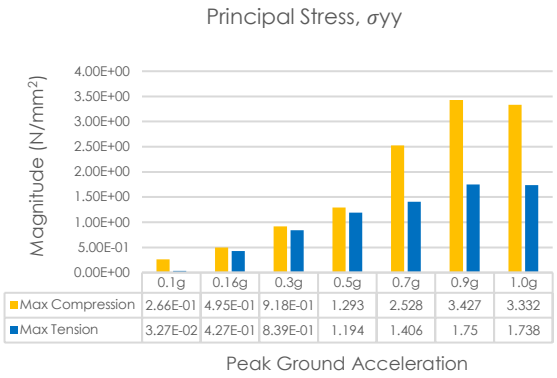

Figure 26 Principal Stress in y direction

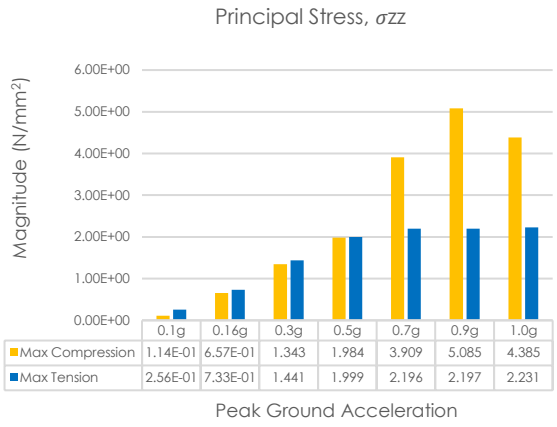

Figure 27 Principal Stress in z direction

Table 6 Summary of Principal Stresses in x-direction

Principal stress	PGA	Magnitude, N/mm²	
		Max Compression	Max Tension
σ_{xx}	0.1g	1.138e-01	2.552e-01
	0.16g	1.199e-01	2.630e-01
	0.3g	1.155e-01	2.637e-01
	0.5g	3.035e-01	3.337e-01
	0.7g	4.967e-01	5.404e-01
	0.9g	6.155e-01	8.136e-01
	1.0g	6.403e-01	6.884e-01

Table 7 Summary of Principal Stresses in y-direction

Principal stress	PGA	Magnitude, N/mm²	
		Max Compression	Max Tension
σ_{yy}	0.1g	2.660e-01	3.272e-02
	0.16g	4.950e-01	4.271e-01
	0.3g	9.182e-01	8.392e-01
	0.5g	1.293	1.194
	0.7g	2.528	1.406
	0.9g	3.427	1.750
	1.0g	3.332	1.738

Table 8 Summary of Principal Stresses in z-direction

Principal stress	PGA	Magnitude, N/mm²	
		Max Compression	Max Tension
σ_{zz}	0.1g	1.141e-01	2.559e-01
	0.16g	6.573e-01	7.329e-01
	0.3g	1.343	1.441
	0.5g	1.984	1.999
	0.7g	3.909	2.196
	0.9g	5.085	2.197
	1.0g	4.385	2.231

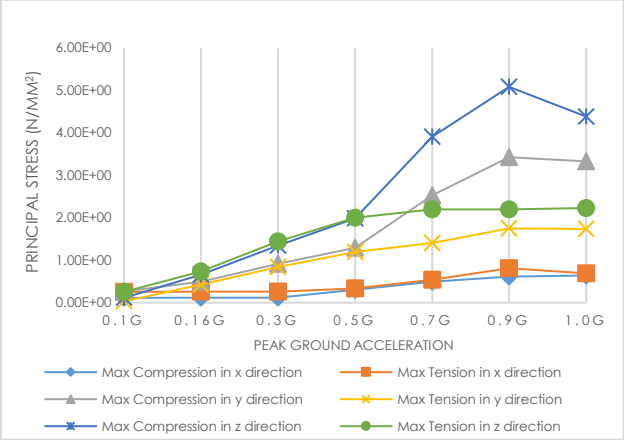

Figure 28 Comparison of Principal Stresses in x, y and z direction

4.0 CONCLUSIONS

In this study, the dynamic time history analysis is completed on one bay three storey low rise school building model under El Centro earthquake with the application of ABAQUS, and the results are presented in contour diagram. Through the simulation, the following conclusion can be drawn:

Firstly, on comparison of the results obtained, it is found that the structure with higher PGA have greater displacement when compared with the structure with lower PGA. From which, the maximum displacements are 1.027 mm, 1.849 mm, 3.047 mm, 5.675 mm, 7.778 mm, 9.603 mm and 10.22 mm for PGA of 0.1g, 0.16g, 0.3g, 0.5g, 0.7g, 0.9g and 1.0g, respectively. By addition of PGA, the local deformation of the structure is increased.

Besides, the Von Mises stress contour diagram of reinforcement bars showed the maximum stress are found in the column near the footing, which are 2.193e+01 N/mm², 3.519e+01 N/mm², 4.892e+01 N/mm², 1.326e+02 N/mm², 2.099e+02 N/mm², 2.606e+02 N/mm² and 2.523e+02 N/mm² for PGA of 0.1g, 0.16g, 0.3g, 0.5g, 0.7g, 0.9g and 1.0g, respectively.

Moreover, the greatest principal stress results in z direction, followed by principal stress in y direction and x direction. In compression, the highest concentration of stress in z direction are 1.141e-01 N/mm², 6.573e-01 N/mm², 1.343 N/mm², 1.984 N/mm², 3.909 N/mm², 5.085 N/mm² and 4.385 N/mm² for PGA of 0.1g, 0.16g, 0.3g, 0.5g, 0.7g, 0.9g and 1.0g, respectively. In tension, the highest concentration of stress in z direction are 2.559e-01 N/mm², 7.329e-01 N/mm², 1.441 N/mm², 1.999 N/mm², 2.196 N/mm², 2.197 N/mm² and 2.231 N/mm² for PGA of 0.1g, 0.16g, 0.3g, 0.5g, 0.7g, 0.9g and 1.0g, respectively. To sum up, S33 > S22 > S11 when the magnitude and sign for each principal stress is considered.

The study conclusively determined that the seismic response of low-rise school buildings significantly varies with changes in peak ground acceleration, highlighting the need for updated design guidelines that incorporate these findings. These results not only challenge existing design practices but also underscore the necessity for more comprehensive seismic analysis in building codes.

Further research is recommended to explore the effects of bi-directional seismic inputs on similar structures and to evaluate the economic implications of implementing advanced seismic safety measures. Additionally, the adoption of new materials and construction techniques that enhance seismic resilience should be investigated to further the development of safer building practices. The exclusion of soil-structure interaction in this analysis represents a simplification that may not capture all aspects of seismic performance, especially in diverse geological conditions. Future studies should consider incorporating SSI to fully understand the interplay between soil properties and structural dynamics, potentially using more advanced modeling techniques that can handle complex interactions between the structure and its foundation.

Acknowledgement

This research was supported by UTAR Research Fund (UTARRF) under Project Number: PSR/RMC/UTARRF/2023-C2/Y02. & Santarli Sdn. Bhd.

Conflicts of Interest

The author(s) declare(s) that there is no conflict of interest regarding the publication of this paper.

References

[1] Hendriyawan. 2007. Seismic Macrozonation of Peninsular Malaysia and Microzonation of Kuala Lumpur City Center and Putrajaya. Degree. Universiti Teknologi Malaysia.

[2] Zibulewsky, J. 2001. Defining Disaster: The Emergency Department Perspective. *Baylor University Medical Center Proceedings.* 14(2): 144-149.

[3] National Research Council. 2003. Preventing Earthquake Disasters: The Grand Challenge in Earthquake Engineering: A Research Agenda for the Network for Earthquake Engineering Simulation (NEES). Washington, DC: The National Academies Press.

[4] Tongkul, F. 2017. Active Tectonics in Sabah – Seismicity and Active Faults. *Bulletin of the Geological Society of Malaysia.* 64: 27-36. Doi: https://doi.org/10.7186/bgsm64201703.

[5] Marto, A., Tan C. S., Kasim F. and Mohd Yunus, N. Z. 2013. Seismic impact in Peninsular Malaysia, The 5th International Geotechnical Symposium-Incheon. 22-24: 237-242. Doi: https://doi.org/10.13140/2.1.3094.9129.

[6] Doocy, S., Daniels, A., Packer, C., Dick, A. and Kirsch, T. D., 2013. The Human Impact of Earthquakes: Historical Review of Events 1980-2009 and Systematic Literature Review. *PLOS Currents.*

[7] Adiyanto, M. I. and Majid, T. A. 2014. Seismic Design of Two Storey Reinforced Concrete Building in Malaysia with Low Class Ductility. *Journal of Engineering Science and Technology*. 9(1): 28-30.

[8] Karadogan, Huseyin & Aydoğan, Mustafa & Girgin, Konuralp & Yuksel, Ercan & Ozer, Nilgun. 2003. Low Rise RC Buildings and the Current Engineering Problems of Seismic Rehabilitation. 10.13140/2.1.2941.9840.

[9] Plevris, V. and Markeset, G. 2018. Educational Challenges in Computer-based Finite Element Analysis and Design of Structures. *Journal of Computer Science*. 14(10): 1351-1362. Doi: 10.3844/jcssp.2018.1351.1362.

[10] National Research Council. 1991. *Improving Engineering Design: Designing for Competitive Advantage*. Washington, DC: The National Academies Press. Doi: 10.17226/1774.

[11] Grzesik, W., Bartoszuk, M. and Nieslony, P. 2005. Finite Element Modelling of Temperature Distribution in the Cutting Zone in Turning Processes with Differently Coated Tools. *Journal of Materials Processing Technology*. 164-165, 1204-1211. Doi: 10.1016/j.jmatprotec.2005.02.136.

[12] Veni, M. N. V, Sitaram, G. and Reddy, M. A. 2017. A Parametric Study on Outer Layer of Helmet using ABAQUS. *International Journal of Engineering and Management Research (IJEMR)*. 7(5): 9-13.

[13] Shahrul, N. M. and Redzuan, A. 2012. Computional Analysis of Reinforced Concrete Slabs Subjected to Impact Loads. *International Journal of Integrated Engineering*. 4(2): 70-76.

[14] Suvranu, D. 2012. *Introduction to Finite Elements: Abaqus Handout*. 1-61.

[15] Melani, A., Khare, R., Dhakal, R. and Mander, J. 2016. Seismic Risk Assessment of Low Rise RC Frame Structure. *Structure*. 5: 13-22.

[16] Vlad, I. 2016. Nonlinear Analysis of Earthquake-induced Vibrations. Master. Aalborg University.

[17] Mosley, B., Bungey, J., and Hulse, R. 2012. *Reinforced Concrete Design to Eurocode* 2. 7th ed. UK: Palgrave Macmillan.

[18] EN 1993-1-1. 2005. Eurocode 3: Design of Steel Structures – Part 1-1: General Rules and Rules for Buildings.

[19] Mills, N. J., Stämpfli, R., Marone, F., & Brühwiler, P. A. 2009. Finite Element Micromechanics Model of Impact Compression of Closed-cell Polymer Foams. *International Journal of Solids and Structures*. 46(3-4): 677-697. Doi: 10.1016/j.ijsolstr.2008.09.012.

[20] Ismail, R., Ibrahim, A. and Adnan, A. 2019. Damage Assessment of Medium-Rise Reinforced Concrete Buildings in Peninsular Malaysia Subjected to Ranau Earthquake. *International Journal of Civil Engineeing and Technology*. 9(7): 881-888.

[21] Adnan, A., Hendriyawan. M. A. and Selvanayagam, B. 2008. Development of Seismic Hazard Maps of East Malaysia. *In: Advances in Earthquake Engineering Application*. Penerbit UTM. 1-18.

[22] Dassault Systèmes. 2014. *Abaqus/CAE User's Guide*. USA: Dassault Systèmes Simulia Corp.

[23] Mengfei, Y. B. S. 2014. Lateral Displacement of Reinforced Concrete Frame Buildings. Degree. The Ohio State University.

[24] Asad, Md. A., Islam, S., and Siddique, M. N. A. 2015. Effect of High Peak Ground Acceleration on the Liquefaction Behaviour of Subsoil and Impact on the Environment. *Journal of Civil Engineering Research*. 5(4): 83-89.

[25] Chen, T., Ma, W., and Wang, J. 2017. Numerical Analysis of Ground Motion Effects in the Loess Regions of Western China. *Shock and Vibration*. 2017: 1-9.

[26] Henning, L. 2012. Simulating Ductile Fracture in Steel using the Finite Element Method: Comparison of Two Methods for Describing Local Instability due to Ductile Fracture. Degree. University of Oslo.

[27] Buttignol, T. E. T., and Almeida, L. C. 2012. Three-dimensional Analysis of Two-pile Caps. *Revista IBRACON de Estruturas e Material.* 5(2): 252-283.

[28] George, W. H. and Thad, V. JR. 1991. The Analysis of Stress and Deformation. United States of America: Division of Engineering and Applied Science, California Institute of Technology.

[29] Marto, A., Soon, T., Kasim, F., & Zurairahetty, N., & Mohd yunus, N. Z. 2013. *Seismic impact in Peninsular Malaysia*. Doi: 10.13140/2.1.3094.9129.

[30] Raheem, S. E. A., Ahmed, M. M. M., Ahmed, M. M., & Abdel-shafy, A. G. A. 2018. Evaluation of Plan Configuration Irregularity Effects on Seismic Response Demands of L-shaped MRF Buildings. *Bulletin of Earthquake Engineering.* 16(3). https://doi.org/10.1007/s10518-018-0319-7.